Second order isothermal desorption kinetics

Y. Lilach, I.M. Danziger and M. Asscher

Department of Physical Chemistry and the Farkas Center for Light Induced Processes, The Hebrew University, Jerusalem 91904, Israel

Received 22 March 2001; accepted 20 June 2001

A new method is presented to analyze recombinative desorption from surfaces in an isothermal mode. The activation energy for desorption obtained this way is accurate as long as it is coverage independent. Second order recombinative desorption experiments of $^{15}N_2$ and D_2 from Ru(001) were used to demonstrate this method. The activation energies were $E_a(N_2) = 48 \pm 2$ kcal/mol and $E_a(D_2) = 22 \pm 1$ kcal/mol for coverages below 0.1 and 0.2 of saturation coverage, respectively. Studying N/Ru(001) provides evidence for bulk nitrogen atoms that slowly diffuse to the surface leading to isotope scrambling.

KEY WORDS: isothermal desorption; second order kinetics; recombinative desorption

1. Introduction

Temperature-programmed desorption (TPD) is one of the basic experimental tools of surface science for the identification of desorbing species, and for obtaining their desorption kinetics. Comprehensive reviews on the subject exist in the literature [1,2]. Many decades after it was first introduced, new methods are still being developed to improve its analytical power, for example FDS (fractional desorption spectroscopy) [3] which utilizes cycles of controlled heating and cooling of the sample, instead of the standard linear heating rates. The complementary approach, namely keeping the system at a fixed temperature for isothermal desorption, was also used in the past for various systems. However, second order desorption kinetics has not yet been addressed. Second order kinetic analysis is hindered by the need to know the exact initial coverage of the desorbing species. We present here a method that circumvents this problem with a simple manipulation of the desorption rate equations.

Determination of the rate of desorption can be achieved either by detecting the desorbing species (usually with a quadrupole mass spectrometer – QMS) or by monitoring the remaining coverage on the surface. Isothermal desorption was employed over the years to analyze desorption kinetics. For example, that of methanol desorption from $Al_2O_3(001)$ [4] where a kinetics order of 0.53 was obtained, the kinetics of CO adsorption and desorption from Pd(110) [5], NH_3/Re(0001) [6] monitored by optical second harmonic generation (SHG) and isothermal desorption of ultrathin silver layers from Ni(111) [7], monitored by Auger electron spectroscopy. In all these examples, first order kinetics govern the desorption process.

2. Method of analysis

Described below is a new way to analyze isothermal recombinative desorption that corresponds to second order desorption kinetics.

Assuming high enough pumping speed, the signal measured by a quadrupole mass spectrometer (QMS) facing a sample is proportional to the rate of desorption:

$$Q \propto -\frac{d\theta}{dt}, \tag{1}$$

where Q is the QMS signal and θ is the fractional surface coverage.

Second order rate processes are defined by the following equations:

$$-\frac{d\theta_t}{dt} = k\theta_t^2, \quad \theta_t = \frac{\theta_0}{1+\theta_0 kt}, \tag{2}$$

where θ_t is the coverage at time t, θ_0 the initial coverage at $t = 0$, and $k = \nu e^{-E_a}/RT_s$ the reaction rate constant (E_a the activation energy for the reaction, ν the preexponent and T_s the surface temperature). In our analysis we assume that both E_a and ν are coverage independent. From equations (1) and (2), one obtains the following:

$$Q \propto -\frac{d\theta_t}{dt} = k\left(\frac{\theta_0}{1+\theta_0 kt}\right)^2, \quad Q = Bk\left(\frac{\theta_0}{1+\theta_0 kt}\right)^2, \tag{3}$$

where B is a proportionality constant defining the number of desorbing molecules. Since the QMS response is not necessarily constant for all masses, B is mass dependent.

The inverse of the square root of Q is given by

$$C(t) = \frac{1}{\sqrt{Q}} = \sqrt{\frac{k}{B}}\,t + \frac{1}{\sqrt{Bk}\,\theta_0}. \tag{4}$$

This equation provides a simple and useful procedure to analyze isothermal desorption data. A straight line is obtained when plotting $C(t)$ *vs.* time, with a slope of $\sqrt{k/B}$, defined here as $\sqrt{k'}$.

The advantage of this procedure is that the kinetic information obtained from the slope is *independent of initial coverage*, in contrast to typical second order kinetic schemes. Once k' is known, a standard Arrhenius analysis provides the

1011-372X/01/0900-0035$19.50/0

activation energy for the recombinative desorption process, by plotting $\ln(k')$ *vs.* $1/T_s$.

3. Experimental

The experiments reported here were performed in a UHV chamber having a base pressure of less then 2×10^{-10} Torr. The Ru(001) sample (oriented within ± 0.1° of the (0001) plane) was resistively heated and stabilized to the desired temperature ±2 K. More details on the UHV chamber, sample preparation and characterization were given elsewhere [8]. Atomic ^{15}N and ^{14}N were accumulated on the surface by initially adsorbing molecular N_2 at 82 K followed by 100 eV electron irradiation. Direct dissociation of nitrogen molecules is impossible due to the extremely small dissociation probability of N_2 on the clean Ru(001) [9]. Atomic nitrogen coverages of up to 10% of a monolayer were obtained using the electron induced dissociation technique. Adsorbed deuterium atoms were readily prepared by exposing the Ru(001) surface (at 82 K) to D_2 *via* a leak valve which backfilled the chamber. A glass shroud with a 4 mm aperture covered the QMS. It was placed 1 mm from the sample to minimize contributions to the TPD spectra and the isothermal desorption from surfaces other than the sample.

4. Results

4.1. N/Ru(001)

Figure 1 (a) and (b) demonstrates a typical isothermal desorption experiment of $^{15}N_2$ from Ru(001). After the adsorption of $^{15}N_2$ at 82 K, and its subsequent partial electron induced dissociation, the sample was heated to 600 K in order to desorb the remaining molecularly adsorbed nitrogen and to stabilize and check the base pressure. The practical temperature range for isothermal desorption in the N/Ru(001) system is between 790 and 940 K. At lower temperatures the signal is below the noise level of our experimental setup. Higher temperatures (higher desorption rates) result in saturation of the detection system and loss of data. These limits can be understood from the TPD line shape as a function of coverage, shown in figure 1(c). Typically two temperatures were chosen in each experiment in order to obtain two independent data points starting from the same initial nitrogen coverage. As stated above, this is possible since the slope extracted from equation (4) is insensitive to the initial coverage. The sample was heated at 12 K/s to the desired temperature, and then stabilized. The desorption was detected by the QMS, which was tuned to mass 30. When the detected signal became constant at the first temperature, the sample was heated to the second (higher) desorption temperature. Between the two measurements a short period of cool-down back to 600 K was necessary to recheck the base pressure (a very important part of the procedure for proper data analysis, as will be further discussed below). Figure 1 shows the results recorded at $T_s = 854$ and 963 K. ((a) QMS signal, (b) sample temperature.)

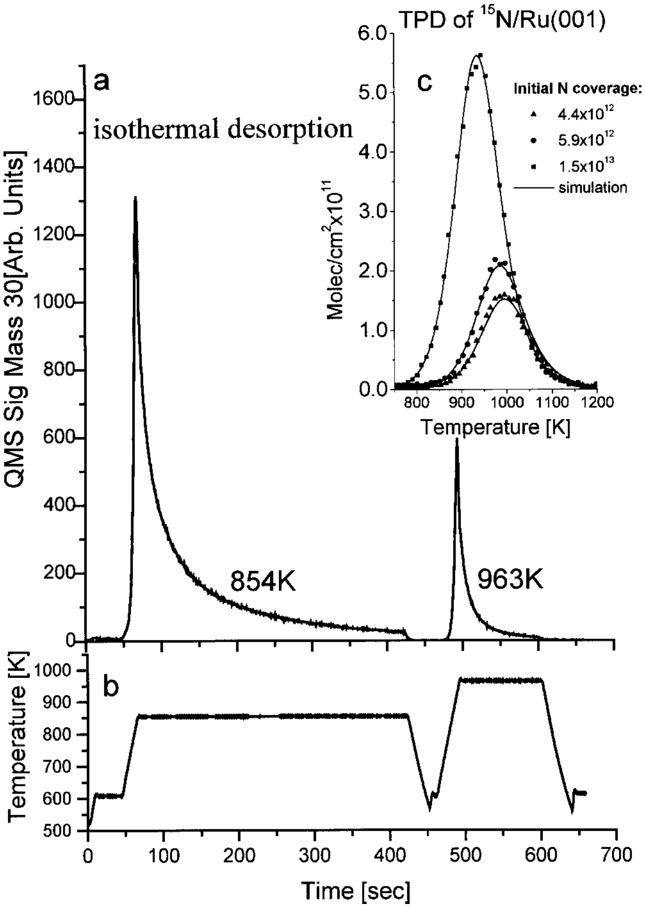

Figure 1. (a) Isothermal desorption data, as detected by the QMS during isothermal recombinative desorption of $^{15}N_2$ from Ru(001) at temperatures 854 and 963 K. (b) The temperature during the desorption process, including the cool-down periods at 600 K. (c) TPD of ^{15}N/Ru(001) for various initial coverages, with heating rate of 2 K/s. The solid lines are obtained from full line-shape simulation, using the following Arrhenius parameters: $\nu = 0.001\,\theta^{-1}$ s^{-1} and $E_a = 48 \pm 2$ kcal/mol.

Analysis of the isothermal desorption curves is done by careful subtraction of the baseline signal and then calculating the inverse of the square root of all the desorption data points. Plots of $1/\sqrt{Q}$ *vs.* time are shown in figure 2. The plots are linear as expected from equations (3) and (4). Deviations from linearity in the first few seconds are most likely due to pumping speed limitations inside the glass shroud. The slopes are proportional to $\sqrt{k'}$.

The intercept of the linear fit is inversely proportional to both $\sqrt{k}$ and the initial coverage θ_0 (see equation (4)). These dependencies tend to affect the intercept in opposite ways. At higher temperature and thus higher k values, the starting coverage is smaller. Since our heating rate is limited to 12 K/s, climbing to higher temperatures implies that a smaller fraction of the initial coverage is left on the surface when the sample temperature is reached and stabilized. Still, k is exponentially dependent on temperature, hence its temperature dependence is stronger and the intercept indeed decreases as temperature increases, as seen in figure 2.

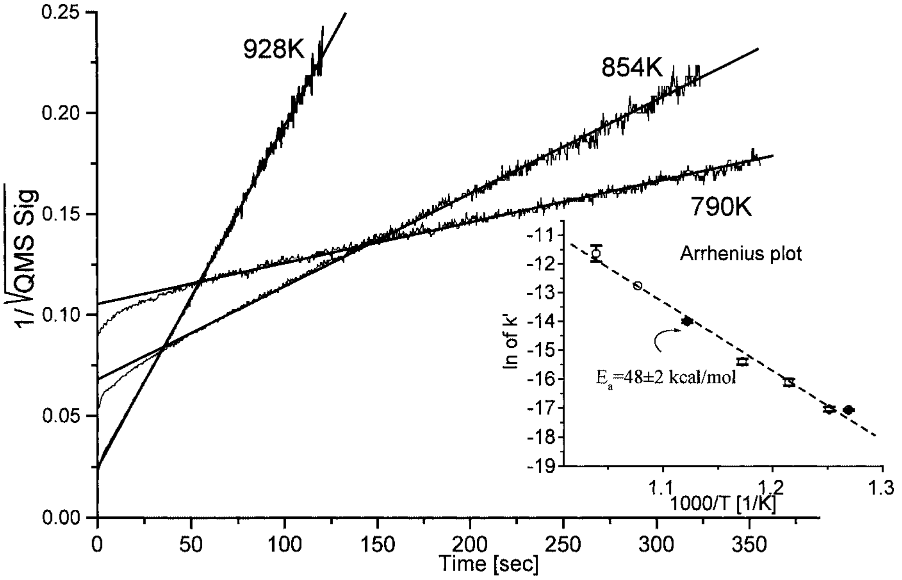

Figure 2. $^{15}N_2$ isothermal recombinative desorption analysis, as described in the text. Note the linearity of the lines as predicted by equation (4). Insert: an Arrhenius plot including all the measured values of k' for nitrogen desorption.

Summary of the resulting slopes for the ^{15}N/Ru(001) system is shown in the insert of figure 2 as an Arrhenius plot, namely ln(k') is plotted *vs.* $1/T$, to obtain the activation energy. It should be noted that there is no need to find the constant B in equation (4), since it does not affect the slope of the Arrhenius plot.

The resulting activation energy for desorption, $E_a = 48 \pm 2$ kcal/mol, is in good agreement with previous results in the literature of 46.2 kcal/mol [10]. This number is practically identical to the activation energy for the reversed process of dissociative adsorption, measured by employing molecular beam techniques [9,11] and later on confirmed by density functional theory calculations [12].

The activation energy parameter can be used as input for a full line-shape analysis of normal TPD spectra, as shown in the insert of figure 1. The same kinetic parameters were used for the fit (±1 kcal/mol) with different initial coverages, resulting in a very good agreement. The error bars in figure 2 are the result of uncertainty in the baseline level during the measurement. In cases where the baseline level was different before and after the isothermal desorption the uncertainty in the measured values increases. Minute changes in the baseline subtraction cause large changes in the resulting slopes. The strong sensitivity to a stable baseline is common to all desorption analysis procedures. Our method has this disadvantage as well, but it enables us to monitor the background/baseline in real time, during the measurements. Therefore one can make a real time estimate of the level of uncertainty. Both TPD and the isothermal desorption data suggest that E_a is independent of coverage below $\theta = 0.1$ ML.

It was previously reported that $^{14}N_2$ and $^{15}N_2$ have different dissociation probability on Ru(001) [11]. It was also proposed that similar isotope effect could be observed in the opposite process – recombinative desorption, provided the molecules *tunnel* through a barrier. We could not, however, observe any difference within our experimental uncertainty between $^{14}N_2$ and $^{15}N_2$ desorption, concluding that the desorption takes place over the barrier, and then no isotope effect is expected [11].

4.2. D/Ru(001)

We have applied our second order isothermal desorption analysis method to D/Ru(001), where higher coverages are easily attainable (up to a full monolayer) by exposure to D_2 gas. This adsorption system has a complex kinetic behavior [13]. The insert in figure 3 shows a series of TPD spectra with coverages up to 1 ML. The range of temperatures used for isothermal desorption experiments were from 290 to 370 K, because of the same considerations mentioned above for the isothermal desorption of nitrogen. A summary of the analysis (the same analysis as described for N_2) of these isotherms is shown in figure 3. A good linear fit of the Arrhenius plot is obtained between 340 and 370 K. These temperatures correspond to coverages up to 0.2 ML. Deuterium coverage determination is possible by adding the integrated area of the isothermal desorption signal to the area of a TPD run performed right after the isotherm (such TPD procedure ensures the desorption of all the remaining D_2).

Activation energy of 22 ± 1 kcal/mol is extracted from the linear part of the Arrhenius plot. The values of the activation energy and the range of linearity we obtained are similar to those reported earlier by Danielson *et al.* [14], but lower than more recent results (28 kcal/mol) obtained at lower coverages by Feulner and Menzel [13]. At lower temperatures (higher coverages) k' becomes only weakly dependent on T_s. The deviation from linearity of the Arrhenius equation suggests lower E_a at higher coverages, or a higher pre-exponent. Isothermal measurements always depend on the net rate, and thus suffer from the typical lack of ability to distinguish be-

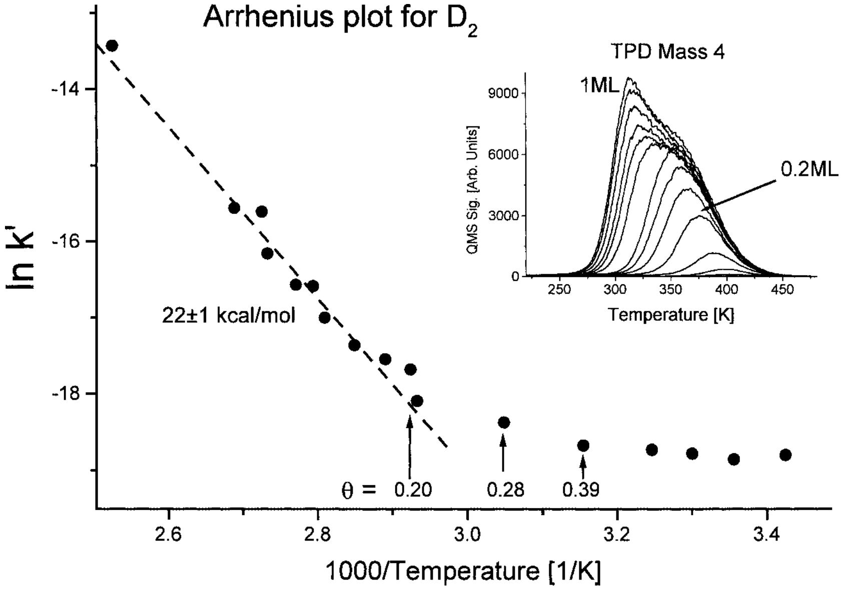

Figure 3. Arrhenius plot for D_2/Ru(001) desorption. Note the deviation from linearity in a temperature which corresponds to $\theta = 0.2$ ML ($T = 340$ K). Higher coverages are indicated by arrows. Insert: TPD of D_2/Ru(001), at a heating rate of 2 K/s with coverages up to 1 ML. The shape of the TPD peak at coverages $\theta > 0.5$ ML is asymmetric, which is a clear indication of the deviation from an ideal second order desorption.

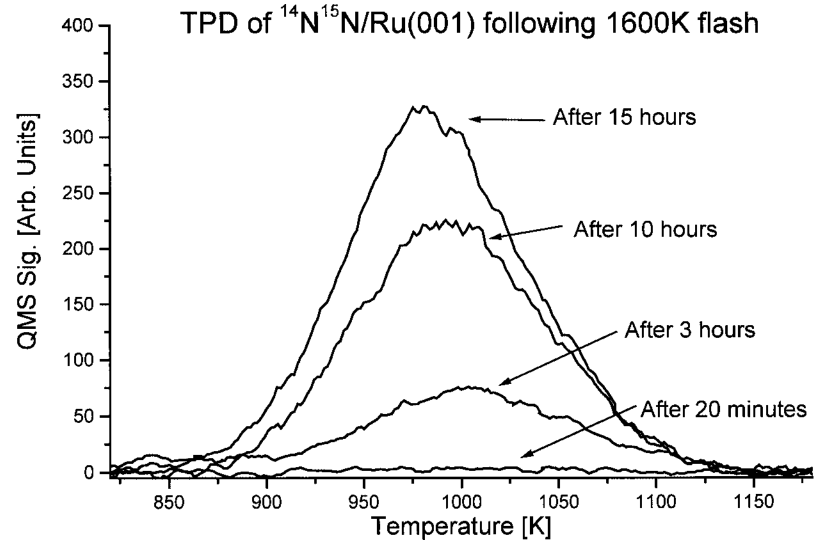

Figure 4. TPD after cleaning the Ru(001) sample by flashing it to 1600 K, shutting all the filaments in the UHV chamber and waiting for the indicated periods of time. Desorption of mass 29 indicates that both ^{14}N and ^{15}N can diffuse into and out of the ruthenium bulk. The heating rate was 9 K/s.

tween the coverage dependencies of E_a and/or of the pre-exponentials. It was also suggested that at higher coverages the desorption is not second order in nature [13,14]. In that case our analysis method has no relevance, since it relies on second order desorption.

4.3. Bulk migration

During the recombinative desorption experiments of $^{15}N_2/^{14}N_2$ from Ru(001), we noticed that after cleaning the sample by flashing it to 1600 K, cooling, and waiting overnight (~10 h), an N_2 TPD peak appeared (masses 29 and 28) at about 950 K, even though no nitrogen was introduced into the system. To further check this observation we repeated the experiment while making sure there was no leak detected and all the filaments in the vacuum system were shut off (to avoid any sources of atomic N due to electron induced dissociation). The results are shown in figure 4 for mass 29. The same phenomenon was observed in a different UHV chamber for ^{14}N/Ru(001). Our interpretation of these results is that nitrogen is slowly emerging from the ruthenium bulk. It diffuses into the bulk during previous exposures and growth of the atomic nitrogen layer. Both carbon and oxygen are known to dissolve into the bulk ruthenium [15], but nitrogen was thought to be immiscible in Ru. Our results clearly suggest that nitrogen atoms reversibly diffuse into and out of the bulk ruthenium. Its rate and temperature dependence are yet undetermined. The bulk diffusion rates are, however, slow enough to avoid a measurable error in the recombinative desorption analysis presented above for the N/Ru system.

5. Conclusions

Using a new method of analysis, we obtained the activation energy for desorption (E_a) for N/Ru(001) and D/Ru(001) of 48 ± 2 and 22 ± 1 kcal/mol, respectively. The method is successfully applicable only when E_a and ν are coverage independent and the desorption follows second order desorption. The strength of the new procedure is in its experimental simplicity and its straightforward data analysis. The method could be useful in studies of surface reactions between coadsorbates in which the surface coverage is not accurately determined.

We also report no isotope effect in the recombinative desorption of N/Ru, and the observation of nitrogen atoms diffusing out of (thus, also into) the bulk ruthenium. This diffusion is very slow, and further study is needed to understand its rate, temperature dependence and mechanism.

Acknowledgement

This work was supported by the Israel Science Foundation and the German–Israel Foundation. The Farkas center is supported by the Bundesministerium für Forschung und Technologie and the Minerva Gesellschaft für die Forschung mbh.

References

[1] D.A. King, Surf. Sci. 47 (1975) 384.
[2] A.M. de Jong and J.W. Niemantsverdriet, Surf. Sci. 233 (1990) 355.
[3] A.J. Franz, J.T. Ranney, W.B. Jackson and J.L. Gland, J. Chem. Phys. B 103 (1999) 4457.
[4] S.Y. Nishimura, R.F. Gibbons and N.J. Tro, J. Phys. Chem. B 102 (1998) 6831.
[5] K.Y. Watanabe and H. Fukutani, J. Chem. Phys. 112 (2000) 7652.
[6] M. Asscher and Z. Rosenzweig, J. Vac. Sci. Technol. A 9 (1991) 1913.
[7] S. Mroz, Z. Jankowski and M. Nowicki, Surf. Sci. 454 (2000) 702.
[8] T. Livneh, Y. Lilach and M. Asscher, J. Chem. Phys. 111 (1999) 11138.
[9] L. Romm, G. Katz, R. Kosloff and M. Asscher, J. Phys. Chem. B 101 (1997) 2213.
[10] L. Diekhoner, A. Baurichter, H. Mortensen and A.C. Luntz, J. Chem. Phys. 112 (2000) 2507.
[11] L. Romm, O. Citri, R. Kosloff and M. Asscher, J. Chem. Phys. 112 (2000) 8221.
[12] M.J. Murphy, J.F. Skelly, A. Hodgson and B. Hammer, J. Chem. Phys. 110 (1999) 6954;
J.J. Mortensen, Y. Morikawa, B. Hammer and J.K. Nørskov, J. Catal. 169 (1997) 85.
[13] P. Feulner and D. Menzel, Surf. Sci. 154 (1985) 489.
[14] L.R. Danielson, M.J. Dresser, E.E. Donaldson and T.J. Dickinson, Surf. Sci. 71 (1978) 599.
[15] C. Stampfl, S. Schwegmann, H. Over, M. Scheffler and G. Ertl, Phys. Rev. Lett. 77 (1996) 3371.